

Search for a Z' at the Z resonance

L3 Collaboration

O. Adrianiⁿ, M. Aguilar-Benitez^w, S. Ahlenⁱ, J. Alcaraz^o, A. Aloisio^z, G. Alverson^j,
M.G. Alvaggi^z, G. Ambrosi^{ae}, Q. An^p, H. Anderhub^{as}, A.L. Anderson^m, V.P. Andreev^{ai},
L. Antonov^{am}, D. Antreasyan^g, P. Arce^w, A. Arefiev^y, A. Atamanchuk^{ai}, T. Azemoon^c,
T. Aziz^{a,h}, P.V.K.S. Baba^p, P. Bagnaia^{ah}, J.A. Bakken^{ag}, L. Baksay^{ao}, R.C. Ball^c, S. Banerjee^h,
J. Bao^e, R. Barilliére^o, L. Barone^{ah}, A. Baschirotto^x, R. Battiston^{ae}, A. Bay^q, F. Becattiniⁿ,
U. Becker^{m,as}, F. Behner^{as}, J. Behrens^{as}, Gy.L. Bencze^k, J. Berdugo^w, P. Berges^m,
B. Bertucci^{ae}, B.L. Betev^{am,as}, M. Biasini^{ae}, A. Biland^{as}, G.M. Bilei^{ae}, R. Bizzarri^{ah},
J.J. Blaising^d, G.J. Bobbink^{o,b}, R. Bock^a, A. Böhm^a, B. Borgia^{ah}, M. Bosetti^x, D. Bourilkov^{ab},
M. Bourquin^q, D. Boutigny^d, B. Bouwens^b, E. Brambilla^z, J.G. Branson^{aj}, I.C. Brock^{af},
M. Brooks^u, A. Bujak^{ap}, J.D. Burger^m, W.J. Burger^q, J. Busenitz^{ao}, A. Buytenhuijs^{ab},
X.D. Cai^p, M. Capell^t, M. Caria^{ae}, G. Carlino^z, A.M. Cartacciⁿ, R. Castello^x, M. Cerrada^w,
F. Cesaroni^{ah}, Y.H. Chang^m, U.K. Chaturvedi^p, M. Chemarin^v, A. Chen^{au}, C. Chen^f,
G.M. Chen^f, H.F. Chen^r, H.S. Chen^f, M. Chen^m, W.Y. Chen^{au}, G. Chiefari^z, C.Y. Chien^e,
M.T. Choi^{an}, S. Chung^m, C. Civininiⁿ, I. Clare^m, R. Clare^m, T.E. Coan^u, H.O. Cohn^{ac},
G. Coignet^d, N. Colino^o, A. Contin^g, X.T. Cui^p, X.Y. Cui^p, T.S. Dai^m, R. D'Alessandroⁿ,
R. de Asmundis^z, A. Degré^d, K. Deiters^{aq}, E. Dénes^k, P. Denes^{ag}, F. DeNotaristefani^{ah},
M. Dhina^{as}, D. DiBitonto^{ao}, M. Diemoz^{ah}, H.R. Dimitrov^{am}, C. Dionisi^{ah,o}, L. Djambazov^{as},
M.T. Dova^p, E. Drago^z, D. Duchesneau^q, P. Duinker^b, I. Duran^{ak}, S. Easo^{ae},
H. El Mamouni^v, A. Engler^{af}, F.J. Eppling^m, F.C. Erné^b, P. Extermann^q, R. Fabbretti^{aq},
M. Fabre^{aq}, S. Falciano^{ah}, S.J. Fan^{al}, O. Fackler^t, J. Fay^v, M. Felcini^o, T. Ferguson^{af},
D. Fernandez^w, G. Fernandez^w, F. Ferroni^{ah}, H. Fesefeldt^a, E. Fiandrini^{ae}, J. Field^q,
F. Filthaut^{ab}, G. Finocchiaro^{ah}, P.H. Fisher^e, G. Forconi^q, T. Foreman^b, K. Freudenreich^{as},
W. Friebel^{ar}, M. Fukushima^m, M. Gailloud^s, Yu. Galaktionov^{y,m}, E. Galloⁿ, S.N. Ganguli^{o,h},
P. Garcia-Abia^w, D. Gele^v, S. Gentile^{ah,o}, S. Goldfarb^j, Z.F. Gong^r, E. Gonzalez^w,
A. Gougas^e, D. Goujon^q, G. Gratta^{ad}, M. Gruenewald^{ad}, C. Gu^p, M. Guanziroli^p, J.K. Guo^{al},
V.K. Gupta^{ag}, A. Gurtu^h, H.R. Gustafson^c, L.J. Gutay^{ap}, K. Hangarter^a, B. Hartmann^a,
A. Hasan^p, D. Hauschildt^b, C.F. He^{al}, J.T. He^f, T. Hebbeker^a, M. Hebert^{aj}, G. Herten^m,
A. Hervé^o, K. Hilgers^a, H. Hofer^{as}, H. Hoorani^q, G. Hu^p, G.Q. Hu^{al}, B. Ille^v, M.M. Ilyas^p,
V. Innocente^o, H. Janssen^o, S. Jezequel^d, B.N. Jin^f, L.W. Jones^c, A. Kasser^s, R.A. Khan^p,
Yu. Kamyshkov^{ac}, P. Kapinos^{ai,ar}, J.S. Kapustinsky^u, Y. Karyotakis^o, M. Kaur^p, S. Khokhar^p,
M.N. Kienzle-Focacci^q, J.K. Kim^{an}, S.C. Kim^{an}, Y.G. Kim^{an}, W.W. Kinnison^u, D. Kirkby^{ad},
S. Kirsch^{ar}, W. Kittel^{ab}, A. Klimentov^{m,y}, A.C. König^{ab}, E. Koffeman^b, O. Kornadt^a,
V. Koutsenko^{m,y}, A. Koulbardis^{ai}, R.W. Kraemer^{af}, T. Kramer^m, V.R. Krastev^{am,ae},
W. Krenz^a, A. Krivshich^{ai}, H. Kuijten^{ab}, K.S. Kumar^l, A. Kunin^{l,y}, G. Landiⁿ, D. Lanske^a,
S. Lanzano^z, P. Lebrun^v, P. Lecomte^{as}, P. Lecoq^o, P. Le Coultre^{as}, D.M. Lee^u, I. Leedom^j,
C. Leggett^c, J.M. Le Goff^o, R. Leiste^{ar}, M. Lentiⁿ, E. Leonardi^{ah}, X. Leytens^b, C. Li^{r,p},
H.T. Li^f, P.J. Li^{al}, J.Y. Liao^{al}, W.T. Lin^{au}, Z.Y. Lin^r, F.L. Linde^o, B. Lindemann^a, L. Lista^z,
Y. Liu^p, W. Lohmann^{ar,o}, E. Longo^{ah}, Y.S. Lu^f, J.M. Lubbers^o, K. Lübelsmeyer^a, C. Luci^{ah},
D. Luckey^{g,m}, L. Ludovici^{ah}, L. Luminari^{ah}, W. Lustermann^{ar}, J.M. Ma^f, W.G. Ma^r,

M. MacDermott^{as}, P.K. Malhotra^{h,l}, R. Malik^p, A. Malinin^y, C. Maña^w, M. Maolinbay^{as}, P. Marchesini^{as}, F. Marion^d, A. Marinⁱ, J.P. Martin^v, L. Martinez-Laso^w, F. Marzano^{ah}, G.G.G. Massaro^b, K. Mazumdar^h, P. McBride^l, T. McMahon^{ap}, D. McNally^{as}, M. Merk^{af}, L. Merola^z, M. Meschiniⁿ, W.J. Metzger^{ab}, Y. Mi^s, G.B. Mills^u, Y. Mir^p, G. Mirabelli^{ah}, J. Mnich^a, M. Möller^a, B. Monteleoniⁿ, R. Morand^d, S. Morganti^{ah}, N.E. Moulai^p, R. Mount^{ad}, S. Müller^a, A. Nadtochy^{ai}, E. Nagy^k, M. Napolitano^z, F. Nessi-Tedaldi^{as}, H. Newman^{ad}, C. Neyer^{as}, M.A. Niaz^p, A. Nippe^a, H. Nowak^{ar}, G. Organtini^{ah}, D. Pandoulas^a, S. Paolettiⁿ, P. Paolucci^z, G. Pascala^{ah}, G. Passaleva^{n,ae}, S. Patricelli^z, T. Paul^e, M. Pauluzzi^{ae}, C. Paus^a, F. Pauss^{as}, Y.J. Pei^a, S. Pensotti^x, D. Perret-Gallix^d, J. Perrier^q, A. Pevsner^e, D. Piccolo^z, M. Pieri^o, P.A. Piroué^{ag}, F. Plasil^{ac}, V. Plyaskin^y, M. Pohl^{as}, V. Pojidaev^{y,n}, H. Postema^m, Z.D. Qi^{al}, J.M. Qian^c, K.N. Qureshi^p, R. Raghavan^h, G. Rahal-Callot^{as}, P.G. Rancoita^x, M. Rattaggi^x, G. Raven^b, P. Razis^{aa}, K. Read^{ac}, D. Ren^{as}, Z. Ren^p, M. Rescigno^{ab}, S. Reucroft^j, A. Ricker^a, S. Riemann^{ar}, B.C. Riemers^{ap}, K. Riles^c, O. Rind^c, H.A. Rizvi^p, F.J. Rodriguez^w, B.P. Roe^c, M. Röhner^a, S. Röhner^a, L. Romero^w, J. Rose^a, S. Rosier-Lees^d, R. Rosmalen^{ab}, Ph. Rosselet^s, W. van Rossum^b, S. Roth^a, A. Rubbia^m, J.A. Rubio^o, H. Rykaczewski^{as}, M. Sachwitz^{ar}, J. Salicio^o, J.M. Salicio^w, G.S. Sanders^u, A. Santocchia^{ae}, M.S. Sarakinos^m, G. Sartorelli^{g,p}, M. Sassowsky^a, G. Sauvage^d, V. Schegelsky^{ai}, D. Schmitz^a, P. Schmitz^a, M. Schneegans^d, H. Schopper^{at}, D.J. Schotanus^{ab}, S. Shotkin^m, H.J. Schreiber^{ar}, J. Shukla^{af}, R. Schulte^a, S. Schulte^a, K. Schultze^a, J. Schwenke^a, G. Schwering^a, C. Sciacca^z, I. Scott^l, R. Sehgal^p, P.G. Seiler^{aq}, J.C. Sens^{o,b}, L. Servoli^{ae}, I. Sheer^{aj}, D.Z. Shen^{al}, S. Shevchenko^{ad}, X.R. Shi^{ad}, E. Shumilov^y, V. Shoutko^y, D. Son^{an}, A. Sopczak^{aj}, C. Spartiotis^e, T. Spickermann^a, P. Spillantiniⁿ, R. Starosta^a, M. Steuer^{g,m}, D.P. Stickland^{ag}, F. Sticazzi^m, H. Stone^{ag}, K. Strauch^l, B.C. Stringfellow^{ap}, K. Sudhakar^h, G. Sultanov^p, L.Z. Sun^{r,p}, H. Suter^{as}, J.D. Swain^p, O. Syben^a, A.A. Syed^{ab}, X.W. Tang^f, L. Taylor^j, G. Terzi^x, Samuel C.C. Ting^m, S.M. Ting^m, M. Tonutti^a, S.C. Tonwar^h, J. Tóth^k, A. Tsaregorodtsev^{ai}, G. Tsipolitis^{af}, C. Tully^{ag}, K.L. Tung^f, J. Ulbricht^{as}, L. Urbán^k, U. Uwer^a, E. Valente^{ah}, R.T. Van de Walle^{ab}, I. Veltlitsky^y, G. Viertel^{as}, P. Vikas^p, U. Vikas^p, M. Vivargent^d, H. Vogel^{af}, H. Vogt^{ar}, I. Vorobiev^y, A.A. Vorobyov^{ai}, L. Vuilleumier^s, M. Wadhwa^d, W. Wallraff^a, C. Wang^m, C.R. Wang^r, G.H. Wang^{af}, X.L. Wang^r, Y.F. Wang^m, Z.M. Wang^{p,r}, A. Weber^a, J. Weber^{as}, R. Weill^s, T.J. Wenaus^t, J. Wenninger^q, M. White^m, C. Willmott^w, F. Wittgenstein^o, D. Wright^{ag}, S.X. Wu^p, B. Wysłouch^m, Y.Y. Xie^{al}, J.G. Xu^f, Z.Z. Xu^r, Z.L. Xue^{al}, D.S. Yan^{al}, B.Z. Yang^r, C.G. Yang^f, G. Yang^p, C.H. Ye^p, J.B. Ye^r, Q. Ye^p, S.C. Yeh^{au}, Z.W. Yin^{al}, J.M. You^p, N. Yunus^p, M. Yzerman^b, C. Zaccardelli^{ad}, P. Zemp^{as}, M. Zeng^p, Y. Zeng^a, D.H. Zhang^b, Z.P. Zhang^{r,p}, B. Zhouⁱ, G.J. Zhou^f, J.F. Zhou^a, R.Y. Zhu^{ad}, A. Zichichi^{g,o,p} and B.C.C. van der Zwaan^b

^a *I. Physikalisches Institut, RWTH, W-5100 Aachen, FRG*²
*III. Physikalisches Institut, RWTH, W-5100 Aachen, FRG*²

^b *National Institute for High Energy Physics, NIKHEF, NL-1009 DB Amsterdam, The Netherlands*

^c *University of Michigan, Ann Arbor, MI 48109, USA*

^d *Laboratoire d'Annecy-le-Vieux de Physique des Particules, LAPP, IN2P3-CNRS,
B.P. 110, F-74941 Annecy-le-Vieux Cedex, France*

^e *Johns Hopkins University, Baltimore, MD 21218, USA*

^f *Institute of High Energy Physics, IHEP, 100039 Beijing, China*

^g *INFN-Sezione di Bologna, I-40126 Bologna, Italy*

^h *Tata Institute of Fundamental Research, Bombay 400 005, India*

ⁱ *Boston University, Boston, MA 02215, USA*

^j *Northeastern University, Boston, MA 02115, USA*

^k *Central Research Institute for Physics of the Hungarian Academy of Sciences, H-1525 Budapest 114, Hungary*³

^l *Harvard University, Cambridge, MA 02139, USA*

- ^m Massachusetts Institute of Technology, Cambridge, MA 02139, USA
- ⁿ INFN Sezione di Firenze and University of Florence, I-50125 Florence, Italy
- ^o European Laboratory for Particle Physics, CERN, CH-1211 Geneva 23, Switzerland
- ^p World Laboratory, FBLJA Project, CH-1211 Geneva 23, Switzerland
- ^q University of Geneva, CH-1211 Geneva 4, Switzerland
- ^r Chinese University of Science and Technology, USTC, Hefei, Anhui 230 029, China
- ^s University of Lausanne, CH-1015 Lausanne, Switzerland
- ^t Lawrence Livermore National Laboratory, Livermore, CA 94550, USA
- ^u Los Alamos National Laboratory, Los Alamos, NM 87544, USA
- ^v Institut de Physique Nucléaire de Lyon, IN2P3-CNRS, Université Claude Bernard, F-69622 Villeurbanne Cedex, France
- ^w Centro de Investigaciones Energeticas, Medioambientales y Tecnologicas, CIEMAT, E-28040 Madrid, Spain
- ^x INFN-Sezione di Milano, I-20133 Milan, Italy
- ^y Institute of Theoretical and Experimental Physics, ITEP, Moscow, Russian Federation
- ^z INFN-Sezione di Napoli and University of Naples, I-80125 Naples, Italy
- ^{aa} Department of Natural Sciences, University of Cyprus, Nicosia, Cyprus
- ^{ab} University of Nymegen and NIKHEF, NL-6525 ED Nymegen, The Netherlands
- ^{ac} Oak Ridge National Laboratory, Oak Ridge, TN 37831, USA
- ^{ad} California Institute of Technology, Pasadena, CA 91125, USA
- ^{ae} INFN-Sezione di Perugia and Università Degli Studi di Perugia, I-06100 Perugia, Italy
- ^{af} Carnegie Mellon University, Pittsburgh, PA 15213, USA
- ^{ag} Princeton University, Princeton, NJ 08544, USA
- ^{ah} INFN-Sezione di Roma and University of Rome, "La Sapienza", I-00185 Rome, Italy
- ^{ai} Nuclear Physics Institute, St. Petersburg, Russian Federation
- ^{aj} University of California, San Diego, CA 92093, USA
- ^{ak} Dept. de Fisica de Particulas Elementales, Univ. de Santiago, E-15706 Santiago de Compostela, Spain
- ^{al} Shanghai Institute of Ceramics, SIC, Shanghai, China
- ^{am} Bulgarian Academy of Sciences, Institute of Mechatronics, BU-1113 Sofia, Bulgaria
- ^{an} Center for High Energy Physics, Korea Advanced Institute of Sciences and Technology, 305-701 Taejon, Republic of Korea
- ^{ao} University of Alabama, Tuscaloosa, AL 35486, USA
- ^{ap} Purdue University, West Lafayette, IN 47907, USA
- ^{aq} Paul Scherrer Institut, PSI, CH-5232 Villigen, Switzerland
- ^{ar} DESY-Institut für Hochenergiephysik, O-1615 Zeuthen, FRG
- ^{as} Eidgenössische Technische Hochschule, ETH Zürich, CH-8093 Zürich, Switzerland
- ^{at} University of Hamburg, W-2000 Hamburg, FRG
- ^{au} High Energy Physics Group, Taiwan, China

Received 8 March 1993

Editor: K. Winter

The search for an additional heavy gauge boson Z' is described. The models considered are based on either a superstring-motivated E_6 or on a left-right symmetry and assume a minimal Higgs sector. Cross sections and asymmetries measured with the L3 detector in the vicinity of the Z resonance during the 1990 and 1991 running periods are used to determine limits on the Z - Z' gauge boson mixing angle and on the Z' mass. For Z' masses above the direct limits, we obtain the following allowed ranges of the mixing angle, θ_M , at the 95% confidence level:

- $0.004 \leq \theta_M \leq 0.015$ for the χ model,
- $-0.003 \leq \theta_M \leq 0.020$ for the ψ model,
- $-0.029 \leq \theta_M \leq 0.010$ for the η model,
- $-0.002 \leq \theta_M \leq 0.015$ for the LR model.

1. Introduction

The successful operation of LEP has allowed a precise measurement of the e^+e^- annihilation cross sections near the Z resonance [1,2]. The experimental results confirm the Standard Model [3] within percent precision. Nevertheless, the Standard Model may be regarded as the low energy limit of a theory which unifies electroweak and strong interactions at higher mass scales. Most of these theories predict additional heavy gauge bosons, Z' , and some models allow Z' bosons with masses detectable at present or future colliders. A mixing of the Z' with the standard Z modifies the Z couplings and changes the Z mass. In addition, propagator effects of the Z' deform the Z resonance shape. Therefore, LEP is the ideal place to measure Z-Z' mixing. Analyses [4] based on previous LEP data, on results of neutrino physics and atomic parity violation bound the Z-Z' mixing angle, θ_M , between -0.01 and 0.01 at 90% confidence level, for most models. The direct search for the Z' performed by the CDF Collaboration [5] excludes Z' masses less than 320 GeV at 95% confidence level, for a restricted range of models.

In this paper we study the reaction

$$e^+e^- \rightarrow \gamma, Z, Z' \rightarrow f\bar{f}(\gamma), \quad (1)$$

where f and \bar{f} denote a fermion-antifermion pair, and extract the allowed range for parameters of an additional heavy gauge boson Z' from the cross section and asymmetry data. For this search we use a total luminosity of 17.2 pb^{-1} (corresponding to roughly 40 000 leptonic and 423 000 hadronic events) collected with the L3 detector in 1990 and 1991.

2. The L3 detector

The L3 detector at LEP covers 99% of the full solid angle. It is designed to measure energy and position of leptons and photons with high precision. A detailed description of the detector and its performance can be found elsewhere [6].

¹ Deceased.

² Supported by the German Bundesministerium für Forschung und Technologie.

³ Supported by the Hungarian OTKA fund under contract number 2970.

The detector consists of a time expansion chamber for the tracking and vertex reconstruction of charged particles, a high resolution electromagnetic calorimeter of 11 000 bismuth germanium oxide (BGO) crystals, a hadron calorimeter with uranium absorber and brass proportional wire chambers and a high precision muon spectrometer, consisting of three layers of multi-wire drift chambers, which measures the muon trajectory 56 times in the bending plane and 8 times in the non-bending direction. A cylindrical array of 30 scintillation counters is installed in the barrel region between the electromagnetic and the hadronic calorimeters. The luminosity of LEP is measured by the luminosity monitor, two electromagnetic calorimeters and two sets of proportional wire chambers, situated symmetrically on either side of the interaction point. Each calorimeter is a finely segmented and azimuthally symmetric array of 304 BGO crystals covering the polar angular range $24.93 < \theta < 69.94 \text{ mrad}$. All detectors are inside a 12 m inner diameter solenoid which provides a uniform magnetic field of 0.5 T along the beam direction.

3. Z lineshape measurements

Operating the LEP storage ring in the vicinity of the Z mass with high luminosity permits a detailed study of the lineshape of the Z resonance. We have performed measurements of the reactions

- (1) $e^+e^- \rightarrow \text{hadrons},$
- (2) $e^+e^- \rightarrow \mu^+\mu^-(\gamma),$
- (3) $e^+e^- \rightarrow \tau^+\tau^-(\gamma),$
- (4) $e^+e^- \rightarrow e^+e^-(\gamma).$

The analysis methods used for these reactions are described elsewhere [1,7]. In tables 1 and 2 we summarize the cross sections and asymmetries determined with the data. These measurements are used for our search for a Z' . Additionally, we include our measurements of the τ polarization [8] and the forward-backward asymmetry of the $b\bar{b}$ and $c\bar{c}$ final states [9] at $\sqrt{s} = 91.222 \text{ GeV}$:

Table 1

Results on the cross sections of leptonic and hadronic final states. σ is the cross section extrapolated to the full solid angle. In case of e^+e^- final states, t channel and interference contributions have been subtracted. The quoted errors exclude the luminosity uncertainty of 0.6%.

Year	\sqrt{s} (GeV)	σ (nb)			
		$e^+e^- \rightarrow e^+e^-$	$e^+e^- \rightarrow \mu^+\mu^-$	$e^+e^- \rightarrow \tau^+\tau^-$	$e^+e^- \rightarrow \text{hadrons}$
1990	88.231	0.188±0.053	0.268±0.033	0.228±0.037	4.53±0.11
	89.236	0.473±0.057	0.387±0.038	0.439±0.047	8.50±0.14
	90.238	1.034±0.082	0.929±0.063	0.920±0.077	18.60±0.25
	91.230	1.462±0.031	1.476±0.028	1.463±0.033	30.38±0.12
	92.226	1.135±0.071	1.115±0.066	1.095±0.078	21.78±0.26
	93.228	0.660±0.048	0.505±0.040	0.599±0.051	12.36±0.16
	94.223	0.348±0.037	0.404±0.036	0.427±0.043	8.20±0.14
	systematic error	0.5%	0.8%	1.5%	0.3%
1991	91.254	1.437±0.023	1.497±0.020	1.505±0.025	30.43±0.10
	88.480	0.291±0.040	0.235±0.021	0.236±0.024	5.17±0.09
	89.470	0.528±0.044	0.478±0.028	0.531±0.035	10.08±0.12
	90.228	0.866±0.053	0.866±0.039	0.885±0.047	18.12±0.18
	91.222	1.484±0.030	1.381±0.026	1.447±0.032	30.26±0.13
	91.967	1.239±0.054	1.165±0.048	1.224±0.059	24.51±0.24
	92.966	0.701±0.040	0.686±0.036	0.641±0.041	14.36±0.16
	93.716	0.486±0.032	0.478±0.028	0.535±0.036	10.02±0.13
systematic error		0.5%	0.5%	0.7%	0.2%

- $\tau_{\text{pol}} = -0.132 \pm 0.026 \pm 0.021$,
- $A_{\text{FB}}^{bb} = 0.086 \pm 0.015 \pm 0.007$,
- $A_{\text{FB}}^{cc} = 0.083 \pm 0.038 \pm 0.027$.

4. Z' models

We concentrate our search for the Z' on two kinds of models which lead to an extension of the Standard Model gauge group and allow a "light" Z' with a mass between 100 GeV and 10 TeV:

- A symmetry breaking of the superstring-inspired E_6 gauge group [10] defines the general case of two additional neutral gauge bosons. We assume that only one of them, Z'^0 , is light enough to be detected:

$$Z'^0 = Z'_\chi \cos \Theta_6 + Z'_\psi \sin \Theta_6. \quad (2)$$

Z'_χ and Z'_ψ are eigenstates associated with the symmetry breaking scheme of the model [10]. The parameter Θ_6 determines the couplings of the heavy boson to fermions and the cases $\Theta_6 = 0, \pi/2$ and

$\arctan \sqrt{5/3} - \pi$ define the χ , ψ and η models. Usually, $-\pi/2 \leq \Theta_6 \leq \pi/2$.

- Left-right symmetric models [11] propose a right-handed $SU(2)_R$ extension of the Standard Model gauge group. The mixing between W_L^\pm and W_R^\pm is neglected and the right-handed neutrinos are assumed to be heavy. The parameter α_{LR} is used to describe the couplings of the heavy boson to fermions:

$$\alpha_{LR} = \sqrt{\frac{\cos^2 \theta_w - \sin^2 \theta_w}{\sin^2 \theta_w}} \frac{g_L}{g_R}, \quad (3)$$

where $g_{L,R}$ are the $SU(2)_{L,R}$ coupling constants and $\sin^2 \theta_w$ is the weak mixing angle. If α_{LR} is at its lower bound, $\sqrt{2/3}$, the left-right symmetric model is identical to the χ model of the E_6 group. The upper bound for α_{LR} , $\alpha_{LR} \simeq 1.53$ for $\sin^2 \theta_w = 0.23$ [1], corresponds to $g_L = g_R$. In the following, we call this special case the LR model.

The mass eigenstates, Z and Z' , are mixtures of the symmetry eigenstates Z^0 of the $SU(2) \times U(1)$ group and Z'^0 of the additional $U(1)$ or $SU(2)_R$ groups.

Table 2

Results on forward-backward asymmetries of leptonic final states. In case of e^+e^- final states, A_{FB} is for the s -channel contribution only and extrapolated to the full solid angle. In case of $\mu^+\mu^-$ final states the asymmetries quoted are for acollinearity $\zeta < 15^\circ$ and in $\tau^+\tau^-$ final states for $\zeta < 14.3^\circ$.

Year	\sqrt{s} (GeV)	A_{FB}		
		$e^+e^- \rightarrow e^+e^-$	$e^+e^- \rightarrow \mu^+\mu^-$	$e^+e^- \rightarrow \tau^+\tau^-$
1990	88.231	-0.034 ± 0.276	-0.39 ± 0.12	-0.42 ± 0.20
	89.236	-0.205 ± 0.161	-0.04 ± 0.11	-0.09 ± 0.15
	90.238	-0.111 ± 0.107	-0.184 ± 0.074	-0.18 ± 0.11
	91.230	-0.023 ± 0.028	0.006 ± 0.021	0.07 ± 0.03
	92.226	0.042 ± 0.085	0.110 ± 0.066	-0.04 ± 0.10
	93.228	0.053 ± 0.094	0.095 ± 0.091	0.11 ± 0.12
	94.223	0.129 ± 0.148	0.134 ± 0.099	0.02 ± 0.13
	systematic error	0.005	0.005	0.01
1991	91.254	0.001 ± 0.020	0.018 ± 0.015	0.037 ± 0.021
	88.480	-0.013 ± 0.157	-0.150 ± 0.100	-0.110 ± 0.130
	89.470	-0.126 ± 0.099	-0.200 ± 0.070	-0.152 ± 0.083
	90.228	-0.100 ± 0.075	-0.041 ± 0.052	-0.137 ± 0.070
	91.222	0.019 ± 0.027	0.013 ± 0.021	-0.032 ± 0.029
	91.967	0.103 ± 0.055	0.060 ± 0.045	0.042 ± 0.063
	92.966	0.098 ± 0.072	0.122 ± 0.058	0.161 ± 0.079
	93.716	0.165 ± 0.085	0.084 ± 0.067	0.058 ± 0.082
systematic error		0.005	0.005	0.006

The mixing is described by a matrix using the mixing angle θ_M :

$$\begin{pmatrix} Z \\ Z' \end{pmatrix} = \begin{pmatrix} \cos \theta_M & \sin \theta_M \\ -\sin \theta_M & \cos \theta_M \end{pmatrix} \begin{pmatrix} Z^0 \\ Z^{0'} \end{pmatrix}. \quad (4)$$

The gauge boson masses m_Z , $m_{Z'}$ are related by the Z - Z' mixing angle θ_M :

$$\tan^2 \theta_M = \frac{m_0^2 - m_Z^2}{m_{Z'}^2 - m_0^2}, \quad (5)$$

$$m_0 = \frac{m_W}{\rho \cos \theta_W}. \quad (6)$$

In the absence of mixing, m_0 is the mass of the standard Z boson. In general, ρ is a free parameter. Here we investigate the case $\rho = 1$, i.e., a Higgs sector restricted to doublets.

As an example, fig. 1 shows contributions of the γ , Z and Z' exchange and their interference for $m_{Z'} = 500$ GeV and $\theta_M = 0.1$ in the χ model. We see that even for Z' masses far outside the LEP energy range, Z - Z' mixing modifies the shape of the Z resonance. Propagator effects of the Z' itself cannot be detected

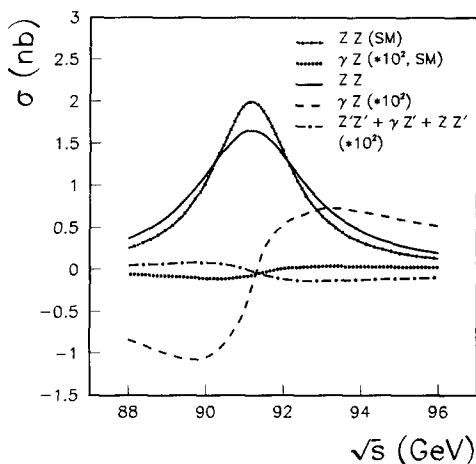


Fig. 1. Born level contributions to $\sigma(e^+e^- \rightarrow \mu^+\mu^-)$ of the ZZ , γZ terms in the Standard Model and the ZZ , γZ and $\gamma Z' + ZZ' + Z'Z$ terms of an assumed Z' in the χ model with $m_{Z'} = 500$ GeV and $\theta_M = 0.1$.

if the mass is high. Therefore, the searches for the Z' at LEP are mainly sensitive to the mixing angle, but not to the Z' mass.

5. Z, Z' lineshape analysis

The determination of limits on θ_M and $m_{Z'}$ in the framework of the above models necessitates a program for the calculation of cross sections and asymmetries that includes all relevant radiative corrections. To allow a comparison and cross check with an analysis without a Z' , we used the program ZEFIT version 3.1 [12] together with the program ZFITTER version 4.5 [13]. ZEFIT is a complement to ZFITTER which contains the modifications to the Z lineshape due to a high mass Z' . Initial and final state QED corrections are considered to $O(\alpha^2)$, higher order corrections for initial state radiation are considered with common photon exponentiation. Weak loop corrections for the Z boson are included to $O(\alpha)$ and are supplemented with the $O(\alpha, \alpha_s)$ and the leading $O(\alpha^2 m_t^4/m_W^4)$ corrections from the top quark insertions in the gauge boson self-energies. Weak loop corrections for the Z' are neglected.

The data listed in tables 1 and 2 have systematic uncertainties in addition to their statistical errors. We consider a partial error correlation when calculating χ^2 ,

$$\chi^2 = \mathcal{A}^T V^{-1} \mathcal{A}, \quad (7)$$

where \mathcal{A} is a column vector with elements such as $(\sigma^{\text{th}} - \sigma^{\text{exp}})$ and $(\mathcal{A}^{\text{th}} - \mathcal{A}^{\text{exp}})$ and V is the $N \times N$ error correlation matrix between measurements. The diagonal elements of V are given by the quadratic sum of the statistical and systematic errors, while the off diagonal elements are given by the product of the common systematic errors. This is generalized to the common systematic error between different data sets. The procedure to implement the LEP energy uncertainty is described in detail elsewhere [14].

6. Results

6.1. Shift of the Z mass

When we include the effects of a possible Z' in a fit to our measurements, the Z mass shifts with respect to the one determined in the Standard Model framework. We fit the mixing angle θ_M and the standard Z mass, m_Z , for different assumed masses $m_{Z'}$. The mass difference

$$\Delta m = m_Z(Z, Z') - m_Z(\text{SM}), \quad (8)$$

where $m_Z(Z, Z')$ is the result of a fit including Z, Z' and mixing, while $m_Z(\text{SM})$ denotes the result of a Standard Model fit, is shown in fig. 2 as a function of $m_{Z'}$ for the χ , ψ , η and LR models. We used our measured value $m_Z(\text{SM}) = (91.195 \pm 0.009)$ GeV [1]. The shift Δm deviates from zero by less than one standard deviation. The increase of m_Z for $m_{Z'} < 500$ GeV is due to both Z-Z' mixing and Z' exchange effects. Above $m_{Z'} = 500$ GeV, m_Z is decreased by Z-Z' mixing since the Z' exchange is negligible. The correlations between θ_M and m_Z or $m_{Z'}$ and m_Z , respectively, are negligible.

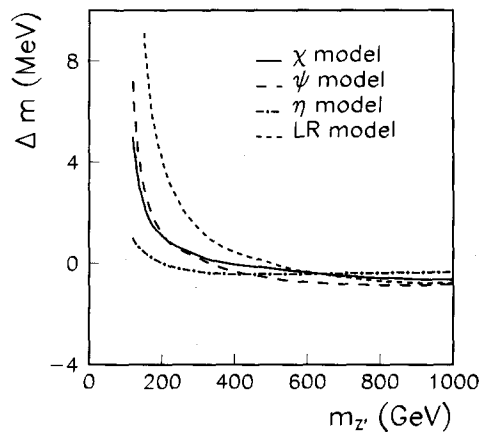


Fig. 2. Difference between the Z mass determined from a Standard Model fit and the mass determined including a potential Z' as well as mixing.

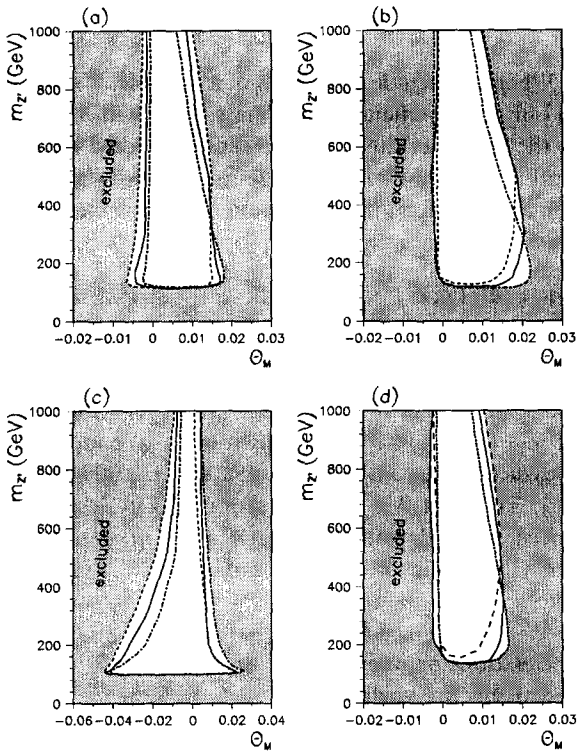


Fig. 3. The 95% CL allowed regions in the $m_{Z'}$ versus θ_M plane in (a) the χ model, (b) the ψ model, (c) the η model and (d) the LR model. The Higgs mass is fixed to $m_H = 300$ GeV. The dashed lines correspond to $m_t = 100$ GeV, the solid lines to $m_t = 150$ GeV and the dash-dotted lines to $m_t = 200$ GeV.

6.2. Limits on θ_M and $m_{Z'}$

In general, the models we consider depend on the following free parameters: m_Z , $m_{Z'}$, θ_M , m_t , m_H , α_s and Z' model parameters such as θ_6 or α_{LR} . In order to reduce the number of free parameters we fix the Higgs mass, $m_H = 100, 300$ and 1000 GeV, the top mass, $m_t = 100, 150$ and 200 GeV and $\alpha_s = 0.12$. The Z mass is limited to the range $m_Z = (91.195 \pm 0.009)$ GeV. Thus, the free parameters are θ_M , $m_{Z'}$ and θ_6 or α_{LR} . First, we compare the cross sections and asymmetries with the predictions of the special E_6 models χ , ψ and η as well as the LR model. In order to determine the allowed regions for the parameters θ_M and $m_{Z'}$ within a particular model we require

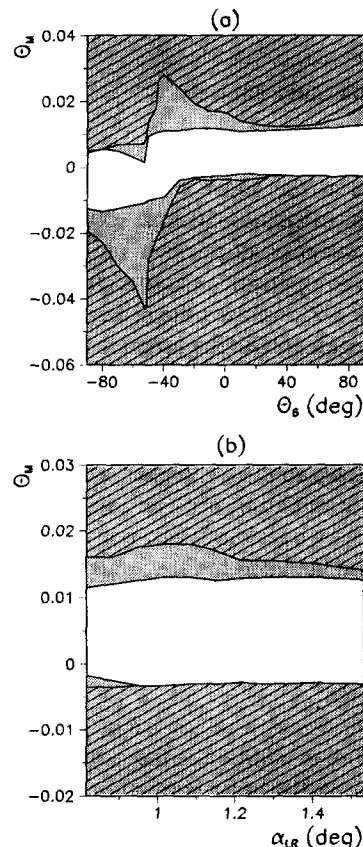


Fig. 4. The 95% CL upper and lower limits of θ_M as a function of the model angle (a) θ_6 for the E_6 model and (b) α_{LR} for the left-right symmetric model. The hatched areas correspond to $m_{Z'} > 200$ GeV and the shaded areas to $m_{Z'} > 700$ GeV. The top and Higgs masses are fixed to $m_t = 150$ GeV and $m_H = 300$ GeV.

$\chi^2 \leq \chi^2_{\min} + 5.99$, corresponding to the 95% confidence limits for two parameters. The results are shown for the χ , ψ , η and LR model in fig. 3. We find only weak dependences of the contours on the top mass.

Fig. 4 shows the 95% CL allowed range of the Z-Z' mixing angle for the whole range of θ_6 and α_{LR} , for the two cases $m_{Z'} > 200$ GeV and > 700 GeV. The top mass and Higgs mass are set to 150 GeV and 300 GeV, respectively. In fig. 5 we compare limits on θ_M and $m_{Z'}$ obtained in the χ model for different values of the Higgs mass ($m_H = 100, 300$ and 1000

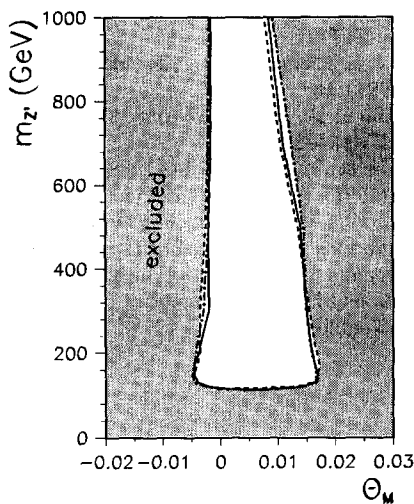


Fig. 5. The 95% CL allowed region in the $m_{Z'}$ versus θ_M plane in the χ model. The dashed lines correspond to $m_H = 100$ GeV, the solid lines to $m_H = 300$ GeV and the dash-dotted lines to $m_H = 1000$ GeV.

GeV). The contours depend weakly on the value of the Higgs mass.

For $m_{Z'}$ above the direct limits [5], we find that the Z-Z' mixing angle is limited, at 95% CL, to the following range:

- $-0.004 \leq \theta_M \leq 0.015$ for the χ model,
- $-0.003 \leq \theta_M \leq 0.020$ for the ψ model,
- $-0.029 \leq \theta_M \leq 0.010$ for the η model,
- $-0.002 \leq \theta_M \leq 0.015$ for the LR model.

We obtain $m_{Z'} > 117$ GeV, 118 GeV, 100 GeV and 130 GeV for the χ , ψ , η and LR models, respectively, at 95% confidence level. All limits take into account the uncertainty of the top mass.

7. Conclusions

The shift of the central value for the mass of the standard Z due to a heavy neutral gauge boson Z' is less than one standard deviation of the present value for m_Z without the Z' .

Our search for a Z' is mainly sensitive to the Z-Z' mixing angle, θ_M . There are no indications for the existence of a Z' ; the fitted Z-Z' mixing angle is compatible with zero for all models considered. Allowed values for the mixing angle are typically between -0.010 and 0.015 at the 95% CL. The influence of the top mass and the Higgs mass on these limits is small. These limits from L3 data substantially improve the existing limits for θ_M [4].

Acknowledgement

We express our gratitude to the CERN accelerator divisions for the excellent performance of the LEP machine. We acknowledge the effort of all engineers and technicians who have participated in the construction and maintenance of this experiment.

References

- [1] L3 Collab., O. Adriani et al., Results from the L3 experiment at LEP, CERN-PPE/93-31, Phys. Rep., to be published.
- [2] ALEPH Collab., D. Decamp et al., Z. Phys. C 53 (1992) 1;
DELPHI Collab., P. Abreu et al., Nucl. Phys. B 367 (1991) 511;
OPAL Collab., P.D. Acton et al., Precision measurements of the neutral current from hadron and lepton production at LEP, CERN-PPE/93-03, submitted to Z. Phys. C.
- [3] S.L. Glashow, Nucl. Phys. 22 (1961) 579;
S. Weinberg, Phys. Rev. Lett. 19 (1967) 1264;
A. Salam, Elementary particle theory, ed. N. Svartholm (Almqvist and Wiksell, Stockholm, 1968) p. 367.
- [4] P. Langacker and M. Luo, Phys. Rev. D 45 (1992) 278;
E. Nardi, E. Roulet and D. Tommasini, Phys. Rev. D 46 (1992) 3040;
F. del Aguila, W. Hollik, J. M. Moreno and M. Quiros, Nucl. Phys. B 372 (1992) 1;
M.C. Gonzalez-Garcia and J.W.F. Valle, Phys. Lett. B 259 (1991) 365;
G. Bhattacharyya et al., Mod. Phys. Lett. A 6 (1991) 2552.
- [5] CDF Collab., F. Abe et al., Phys. Rev. Lett. 68 (1992) 1463.
- [6] L3 Collab., B. Adeva et al., Nucl. Instrum. Methods A 289 (1990) 35.
- [7] L3 Collab., B. Adeva et al., Z. Phys. C 51 (1991) 179.
- [8] L3 Collab., O. Adriani et al., Phys. Lett. B 292 (1992) 454.

- [9] L3 Collab., O. Adriani et al., Phys. Lett. B 294 (1992) 466.
- [10] R.W. Robinett, Phys. Rev. D 26 (1982) 2388;
R.W. Robinett and J.L. Rosner, Phys. Rev. D 26 (1982) 2396;
D. London and J.L. Rosner, Phys. Rep. 34 (1986) 1530;
G. Belanger and S. Godfrey, Phys. Rev. D 35 (1987) 378.
- [11] R.W. Robinett and J.L. Rosner, Phys. Rev. D 25 (1982) 3036; D 27 (1983) 679 (E);
C.N. Leung and J.L. Rosner, Phys. Rev. D 29 (1982) 2132.
- [12] A. Leike, S. Riemann and T. Riemann, University of Munich preprint LMU-91/06, and FORTRAN program ZEFIT;
A. Leike, S. Riemann and T. Riemann, Phys. Lett. B 291 (1992) 187.
- [13] D. Bardin et al., FORTRAN program ZFITTER, and CERN TH/6443-92;
D. Bardin et al., Z. Phys. C 44 (1989) 493; Nucl. Phys. B 351 (1991) 1; Phys. Lett. B 255 (1991) 290.
- [14] The working group on LEP energy and the LEP Collaborations ALEPH, DELPHI, L3 and OPAL, Measurement of the mass of the Z and the energy calibration of LEP, CERN preprint (1993), Phys. Lett. B, to be published.